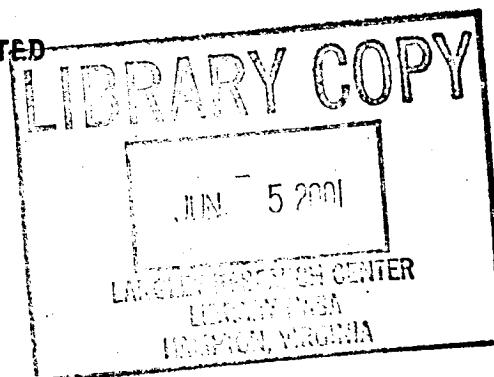NASA-CR-159300

NASA CONTRACTOR REPORT 159300

AN ANALYSIS METHOD FOR MULTI-COMPONENT AIRFOILS

IN SEPARATED FLOW

B.M. RAO, F.A. DVORAK AND B. MASKEW
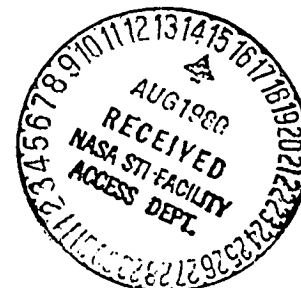
ANALYTICAL METHODS, INCORPORATED
BELLEVUE, WASHINGTON 98004

NF01096

NASA

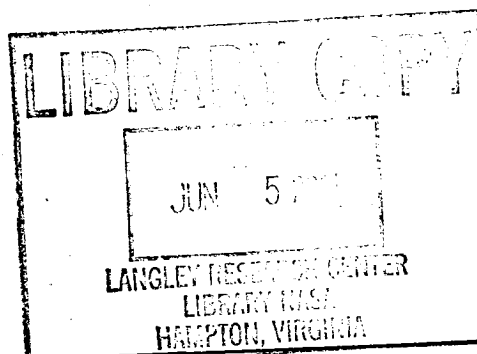National Aeronautics and
Space Administration

Langley Research Center
Hampton, Virginia 23665

NASA CR-159300

1. Report No.	2. Government Accession No.	3. Recipient's Catalog No.
NASA CR-159300		
4. Title and Subtitle		5. Report Date
AN ANALYSIS METHOD FOR MULTI-COMPONENT AIRFOILS IN SEPARATED FLOW		August 1980
		6. Performing Organization Code
7. Author(s)		8. Performing Organization Report No.
B.M. Rao, F.A. Dvorak and B. Maskew		
		10. Work Unit No.
9. Performing Organization Name and Address		
Analytical Methods, Inc. 100 - 116th Avenue S.E. Bellevue, Washington 98004		11. Contract or Grant No.
		NAS1-15729
		13. Type of Report and Period Covered
12. Sponsoring Agency Name and Address		Contractor Report
National Aeronautics and Space Administration Washington, D.C. 20546		14. Sponsoring Agency Code

15. Supplementary Notes

Contract Monitor: Mr. Harry L. Morgan, Jr., NASA Langley Research Center

16. Abstract

The multi-component airfoil program (Langley-MCARF) for attached flow is modified to accept the free vortex sheet separation-flow model program (Analytical Methods, Inc.-CLMAX). The viscous effects are incorporated into the calculation by representing the boundary layer displacement thickness with an appropriate source distribution. The separation flow model incorporated into MCARF has been applied to single component airfoils. Calculated pressure distributions for angles of attack up to the stall are in close agreement with experimental measurements. Even at higher angles of attack beyond the stall, correct trends of separation, decrease in lift coefficients, and increase in pitching moment coefficients are predicted.

17. Key Words (Suggested by Author(s))	18. Distribution Statement
Aerodynamics Separated Flows Multi-Component Airfoils	Unclassified--Unlimited

19. Security Classif. (of this report)	20. Security Classif. (of this page)	21. No. of Pages	22. Price*
Unclassified	Unclassified	38	

N-305

SUMMARY

The multi-component airfoil program (MCARF) for attached flow is modified to accept the free vortex sheet separation flow model of the AMI CLMAX program. The viscous effects are incorporated into the calculation by representing the boundary layer displacement thickness with an appropriate source distribution.

The separation flow model incorporated into MCARF has been applied to single component airfoils. Calculated pressure distributions for angles of attack up to the stall are in close agreement with experimental measurements. Even at higher angles of attack beyond the stall, correct trends of separation, decrease in lift coefficients, and increase in pitching moment coefficients are predicted.

Although the program is designed to handle multi-component airfoils with separation at the trailing component only, multi-component airfoils have not been checked out. It is suggested a better separation criterion such as the method of Nash and Hicks be incorporated into the model as opposed to the present method of Truckenbrodt.

TABLE OF CONTENTS

LIST OF FIGURES

1.0 INTRODUCTION

1.1 Background

During the final design phase of an airfoil, it is essential to include the viscous as well as separation effects at high angles of attack for the accurate evaluation of the aerodynamic performance. No general, mathematically closed form solution presently exists which describes the viscous separated flows around an airfoil. The availability of high-speed large capacity computers and the recent advancements in the potential flow and boundary layer computations has enabled the development of several computer programs which are based on iterative procedures between the viscous/potential flow solutions for attached as well as separated flows.

In Reference 1, a computerized analytical model which computes the performance characteristics of multi-element airfoils in subsonic, viscous flow has been developed under a NASA contract to the Lockheed-Georgia Company. The model computes the viscous pressure distributions, lifts, moments and local boundary layer properties on each element of an arbitrarily arranged slotted airfoil in attached flow. The final viscous solution is obtained by an iterative technique by successively combining the potential flow solution with boundary layer displacement thickness. The details of the model and the computer program (MCARF) are presented in the next section.

Multi-component airfoils operating at high angles of attack will usually experience regions of trailing-edge separation on the upper surfaces of one or more components. At low angles of attack, the cove regions of one or more components may contain a closed separation bubble which can reduce the effectiveness of the downstream slot flow. In either situation, the performance of the system is reduced from that which would be expected with completely attached flow. In practice, some amount of separation is to be expected, and there is a need, therefore, for the capability to predict the performance of multi-component systems having regions of separated flow.

Until recently, our ability to model separation was limited to models that simulated separation by source distributions employing the assumption that the pressure everywhere in the separated region is constant (Ref. 2). None of the methods calculate the pressue in the separation region directly, but rely on some criterion to determine the separated flow

1

pressure level. In general, the methods predict the upstream pressure distributions in a satisfactory manner once a suitable source "outflow" has been chosen.

More recent approaches (Refs. 3 and 4) employ an inverse method to determine the effective airfoil shape to achieve constant pressure in the separated flow region. There is some question as to the uniqueness of the solutions obtained by this procedure. Since none of the methods use a physically realistic wake model, it is difficult to see their applicability in the stall region where a direct analysis procedure for the prediction of aerodynamic characteristics of airfoils is desired.

A procedure which does employ a realistic wake model for separated flow is described in Reference 5. This method, developed by Analytical Methods personnel, uses free vortex sheets to separate the free stream fluid from the wake region (a region of lower total pressure). The strength of each vortex sheet and its location are determined as part of the overall calculation. The procedure allows for a direct calculation of pressures in the separated flow region. The details of the analysis and the computer program (CLMAX) are presented in the next section.

1.2 Present Approach

The primary objective of the present work is to modify the MCARF program to accept the free vortex sheet separation model developed for the CLMAX program. The viscous effects are incorporated into the calculation by representing the boundary layer displacement thickness with an appropriate source distribution over the airfoil surface. This approach enabled incorporation of the separation wake model into MCARF with a minor modification to MCARF, since it does not change the panel geometry of the airfoil surface. For the present study, the program is capable of analyzing a multi-component configuration with separation only on one of the components, presumably the trailing component. The effect of the separated region will, of course, impact the flow around the other components.

The inclusion of the separation model into MCARF involves the development of two iteration loops. The inner (wake) iteration loop for the potential flow relaxes the wake shape for a prescribed separation position, while the outer (viscous/potential flow) iteration loop predicts the separation point location and the displacement thickness distribution from the boundary layer analysis for each of the components.

2

2.0 NOMENCLATURE

A   Aerodynamic influence coefficient

C   Chord length

C_p Pressure coefficient

C_ℓ Lift coefficient

C_m Moment coefficient about the quarter-chord axis

H_{sep} The value of the boundary layer shape factor at which the flow is assumed to separate

IPOT   Choice of potential flow index

ITR   Viscous/potential flow iteration index

ITRW   Wake shape (inner) iteration index

ITRWMX   Maximum number of wake shape iterations

K   Kernel function

N   Number of panels

s   Coordinate along airfoil surface

V   Velocity

WL   Wake length

WF   Wake fineness ratio

x,z   Cartesian coordinates

α Angle of attack

ψ Stream function

γ Vorticity strength

ρ Density

ΔH Increase in total pressure in the separation region

3.0 DESCRIPTION OF COMPUTATIONAL MODELS AND PROGRAMS

3.1 Multi-Component Airfoil (MCARF) Program

In this section, a brief description of a computerized analytical model and the computer program (Ref. 1) which predicts the performance characteristics of the multi-element airfoil in attached, subsonic viscous flow are presented. The model computes the viscous pressure distributions, lift and moments, and boundary layer properties on each element of an arbitrarily arranged slotted airfoil. The final viscous solution is obtained by an iterative technique which combines an inviscid solution with the boundary layer displacement thickness. The surface of each element is approximated as a closed polygon with segments represented by distributed vortex singularities. The boundary layer solution is comprised of mathematical models representing state-of-the-art technology for laminar, transition, and turbulent boundary layers. An additional boundary layer model has been incorporated to compute the characteristics of a confluent boundary layer which reflects the merging of the upper-surface boundary layer with the slot efflux.

3.1.1 Program Operation and Capabilities

The airfoil program is composed of three main parts: (1) geometry specification; (2) potential flow; and (3) boundary layer. After data input and geometry specification, the program enters an iterative cycle which involves the determination of the interrelationship between the potential flow and the boundary layer. After each iteration, a convergence check is made which consists of a simple comparison of the computed lift coefficients. Experience has shown five iterations are necessary to obtain a converged solution. This rapid convergence can be attributed to the iterative technique in which the physical geometry of the airfoil at each iteration is modified taking into account boundary layer thickness computed from the previous iteration.

The program input is kept as simple as possible to make it more user oriented. The coordinates of each element of a multi-element airfoil can be input with respect to a separate coordinate system and are easily positioned relative to other elements by specifying the pivot location and deflection of the element. The boundary layer transition (laminar to turbulent) location can be input as either fixed or free. The total number of calculation points at which the pressures are

4

desired can be input. During a single machine pass, the angle of attack and Mach number can be varied for a constant Reynolds number, Prandtl number, and stagnation temperature. The Karman-Tsien pressure law is employed to represent the compressibility effects. The laminar and turbulent boundary layer routines contain methods to predict boundary layer separation but do not contain methods to model the flow after separation. Therefore, the angle of attack should be limited to that producing attached flows only.

3.1.2 Program Theory

Potential Flow Solution

The program uses a singularity distribution method of Oeller's (Ref. 6), which employs stream functions. The stream functions for a uniform free stream plus that of the vortex sheet is to be a constant on the airfoil surface. This condi-tion is represented mathematically by the Fredholm integral equation

$$\psi + \frac{1}{2\pi} \int_0^{s_{te}} \gamma(\xi) \ln \left[r(s,\xi) \right] d\xi$$

$$= U_\infty x(s) \cos(\alpha) - U_\infty z(s) \sin(\alpha)$$

(3.1)

where ψ is the unknown stream function constant, $r(s,\xi)$ is the distance between two points on the airfoil surface, $x(s)$ and $z(s)$ are coordinates of a point on the surface, and $\gamma(\xi)$ is vortex strength at a point. By dividing the surface into N segments and assuming constant vortex strength for each segment

5

Equation (3.2) becomes

$$\psi - \sum_{j=1}^{N} A_{ij}\gamma_j = U_\infty \left[x_i \cos(\alpha) - z_i \sin(\alpha) \right] \qquad (3.2)$$

where the influence coefficient, A_{ij} is the velocity induced at the jth segment due to a unit vorticity at the ith segment. By specifying a control point at the midpoint of each segment, the influence coefficient becomes an analytic expression. To determine the vortex strength $(\overline{\gamma})$ at the intersection of two segments, the following interpolation formula is used.

$$\overline{\gamma}_j = \frac{\gamma_{j-1}\left(s_j - s_{j-1}\right) + \gamma_j\left(s_{j+1} - s_j\right)}{s_{j+1} - s_{j-1}} \qquad (3.3)$$

For this method, an additional equation is needed to obtain an N by N system of equations. (The unknowns are N-1 number of γ's and ψ). A special Kutta condition is used to reduce the oscillations of the vortex strengths caused by a too close spacing near the trailing edge. This Kutta condition simply requires that the vortex strengths, $(\overline{\gamma})$, vary quadratically for the last four segment corners near the upper and lower surface of the trailing edge and that at the trailing edge

$$(3.4)$$

$$(\overline{\gamma}_1)_l = - (\overline{\gamma}_N)_u$$

Oeller's method combined with this new Kutta condition provided convergent solutions even for cusp-edged as well as supercritical airfoils.

Boundary Layer Solution

The pressure coefficients computed in the potential flow portion of the airfoil program are corrected to account for compressibility with the Karman-Tsien correction law. Using the isentropic flow relations, the local Mach number is computed

and input to the boundary layer portion of the program. The boundary layer consists of an ordinary boundary layer and a confluent boundary layer. The ordinary boundary layer is composed of laminar, transition, and turbulent regions. The confluent boundary layer model was developed by Goradia (Ref. 7) and is one of the unique features of this program.

A flat-plate boundary layer analysis is performed on each surface of an airfoil element, and the leading-edge stagnation point is the plate leading edge. An initial laminar boundary layer region exists from the stagnation point to the point of transition from laminar to turbulent. The laminar boundary layer model used is the method of Cohen and Reshotko (Ref. 8). After computing the laminar boundary layer characteristics at a discrete point, routine BLTRAN is called to check for transition and, if transition has occurred, to check for the formation of a long or short transition bubble and for laminar stall. An initial check is made to determine if the laminar boundary layer is stable or unstable based on the instability criterion established by Schlicting and Ulrich (Ref. 9). If the boundary layer is unstable, a transition check is made based on an empricially derived transition prediction curve. If transition has occurred, the initial quantities needed to start the turbulent calculations are computed. If transition has not occurred, the formation of either a long bubble with corresponding laminar stall or a short bubble with corresponding reattaching is obtained. The user can input a fixed transition location and a check will be made at the beginning of BLTRAN to determine whether or not the fixed location has been reached.

After computing the transition location and the corresponding initial boundary layer properties, the turbulent boundary layer calculations are made using the modified Truckenbrodt method (Ref. 10). If a slot exit plane is reached during the turbulent boundary layer computations, the confluent boundary layer computation is initiated. The confluent boundary layer is a result of the mixing between the slot efflux and the wake from the forward element, and can exist from the slot exit to the trailing edge of the element, depending upon the pressure distribution. The confluent boundary layer formulated by Goradia (Ref. 7) is based on the assumption that the merging of the fore and aft element boundary layers will have "similar" velocity profiles if nondimensionalized in a way analogous to that for a free jet flow.

Equivalent Airfoil Geometry

The airfoil program uses an iterative porcedure to obtain the viscous solution and the basic steps are as follows.

(1) Compute a potential flow solution for the basic airfoil.

(2) Compute boundary layer properties based on the potential flow solution.

(3) Modify the airfoil camber and thickness distributions using the boundary layer displacement thickness.

(4) Compute the aerodynamic performance coefficients.

(5) Repeat steps (1) through (4) until convergence of the performance coefficients is obtained.

In the present version of the program, another option in which the viscous effects are taken into account with the appropriate source distributions to represent the boundary layer thickness is available. This option, if used, does not involve the computation of equivalent airfoil geometry.

3.2 CLMAX Program

In this section a method for calculating the flow about airfoils up to and beyond the stall is described. It is an iterative procedure between potential flow and boundary layer solutions. The separation region is modeled in the potential flow analysis using free vortex sheets which require an inner iteration to estalish their shapes.

3.2.1 Description of the Flow Model

A flow field with separation is shown in Figure 1. Several regions are identifiable.

Region 1: The Potential Flow Region

The region exterior to the boundary layer and separated wake is almost precisely irrotational since the shear is everywhere so low that viscous stresses impart a negligible rotation to the fluid.

Region 1 - Potential Flow Region
Region 2 - Boundary Layer
Region 3 - Free Shear Layer
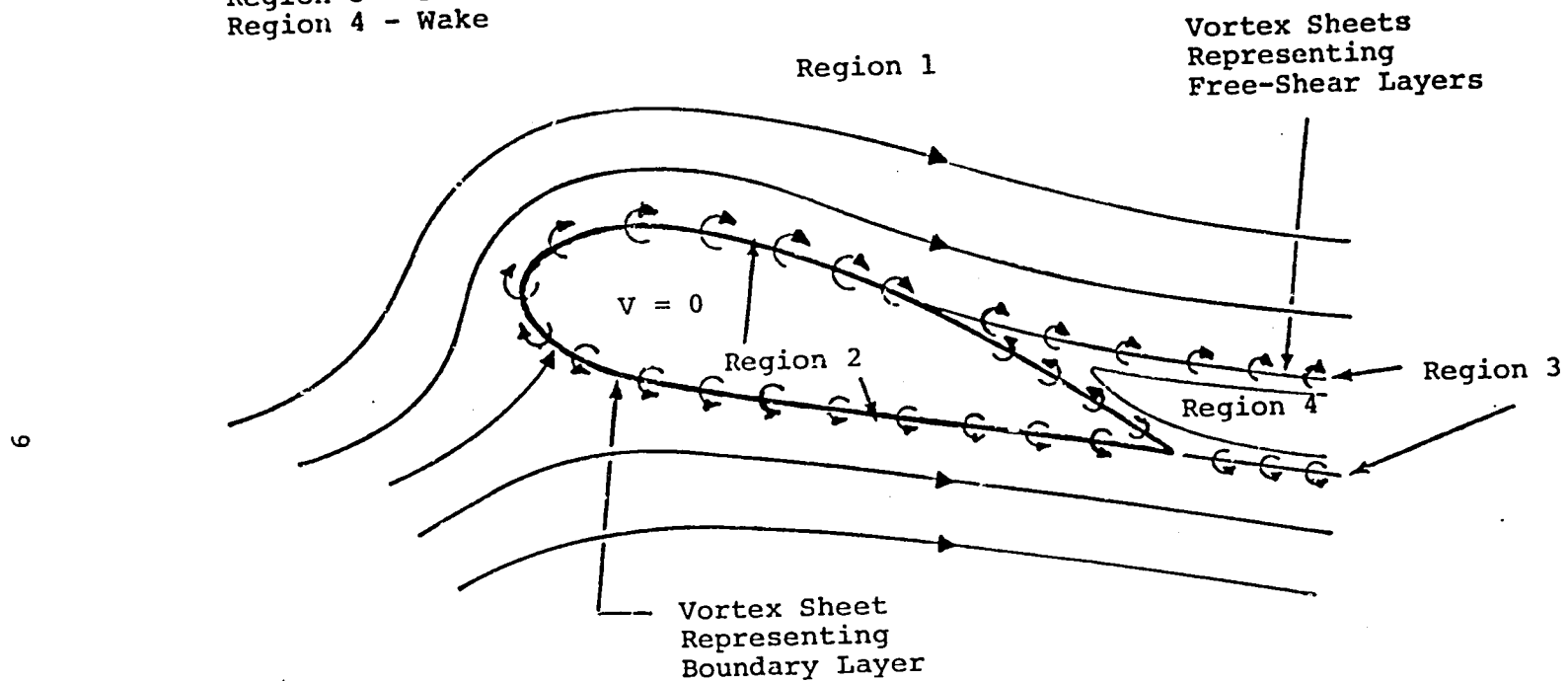Region 4 - Wake

FIGURE 1.   MATHEMATICAL FLOW MODEL

Region 2: The Boundary Layer

The thin region next to the airfoil surface has high shear, and hence, viscous stresses which create significant vorticity.

Region 3: The Free Shear Layer

The thin flow region fed by the separating boundary layer has rotation, but only moderate shear. The vorticity transport is predominantly by convection, although diffusion is not insignificant.

Region 4: The Wake

The wake between the two shed boundary layers is a region with low vorticity and insignificant viscous stresses.

Basic Assumptions

An approximate model of the flow is defined by these assumptions.

(1) The boundary layer and free shear layers do not have significant thickness and, hence, can be represented as slip surfaces; that is, streamlines across which there exists a jump in velocity.

(2) The wake does not have significant vorticity and has constant total pressure. It is, therefore, taken to be a potential flow region.

The flow field car be constructed by adding to the uniform stream the so-called "induced" velocities associated with a vorticity distribution with a strength equal to the curl of the velocity field. To apply this method, the flow must be defined everywhere. The velocity will be zero everywhere inside the airfoil surface. Figure 1 shows the resulting flow which is everywhere irrotational except along sheets where the boundary layer and free shear layers have been squeezed to zero thickness.

The mathematical problem is to find the vorticity sheet strength such that the appropriate boundary conditions are met. The position of the vorticity sheet representing the free shear layer is not known a priori.

Boundary Conditions

The boundary condition for the airfoil surface is flow tangency or

$$\vec{V} \cdot \vec{n} = 0 \tag{3.5}$$

where $\vec{n}$ = unit normal vector, and $\vec{V}$ is the total vorticity vector.

When allowing the boundary layer displacement effect, the right side of this equation will be non-zero.

The free vorticity sheets are located on streamlines and there is no static pressure drop across them.

Approximations for the Free Shear Layer

(1) Wake Shape

Initially, the streamlines are not known and so the shapes of free shear layers must be obtained iteratively, starting from an initial assumption. Earlier calculations in which the vortex sheet shapes were obtained by iteration suggested the initial shape shown in Figure 2, which is incorporated as the basic wake in the program. The upper and lower sheets are represented by parabolic curves passing from the separation points common to a point downstream. The slope at the upstream end is the mean between the free stream direction and the local surface slope. The common point downstream is positioned on the mean wake line, distance WL downstream from the wake midpoint (Figure 2).

(2) Wake Length

Early calculations indicated that the results were sensitive to the length of the free vortex sheets. Good correlation with experimental results was obtained only with relatively short wakes; i.e., wakes extending 0.1c to 0.2c beyond the trailing edge. Several ways of defining the wake length, WL, have been investigated for a number of different airfoils. The final model adopted is based on a "fineness ratio" of the wake; i.e., WL is obtained by multiplying the "height" of the wake (Figure 2) by the wake fineness ratio, WF.
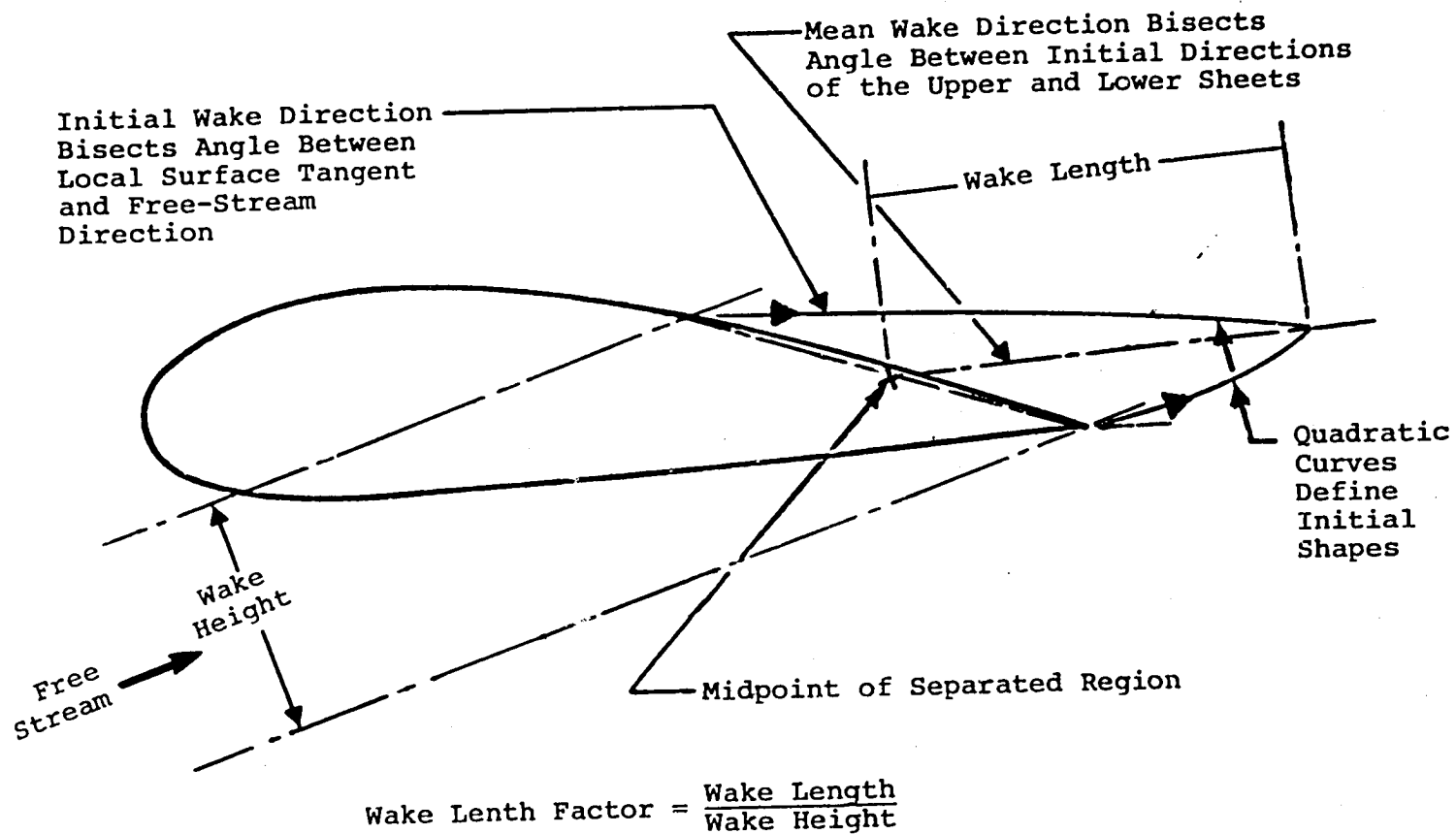
FIGURE 2. INITIAL WAKE GEOMETRY

(3) Wake Pressure

The approximation of the static pressure drop across the free shear layer is used to obtain an expression for the total pressure in the wake in terms of the strength of the free vortex sheets. Considering the upper shear layer, if the average velocity in the layer is denoted by

$$V = \tfrac{1}{2}\left(V_{outer} + V_{inner}\right) \tag{3.6}$$

then

$$V_{outer} = \overline{V} + \gamma_U/2, \text{ and}$$

$$V_{inner} = \overline{V} - \gamma_U/2,$$

since the vorticity, $\gamma_U = V_{outer} - V_{inner}$, on the upper sheet. (The vorticity in the lower shear layer is $\gamma_L = V_{inner} - V_{outer}$.) The jump in total pressure across the shear layer is then

$$\Delta H = H_{inner} - H_{outer}$$

$$= \left\{ P_{inner} + \tfrac{1}{2}\rho\left(\overline{V} - \gamma_U/2\right)^2 \right\}$$

$$- \left\{ P_{outer} + \tfrac{1}{2}\rho\left(\overline{V} + \gamma_U/2\right)^2 \right\}$$

$$= -\rho\overline{V}\gamma_U = \rho\overline{V}\gamma_L \tag{3.7}$$

given the boundary condition that the static pressure, p, has no jump in value across the shear layer.

Since the wake has constant total pressure (assumption (2)), the jump in total pressure across the free shear layer is the same everywhere.

13

3.2.2 Potential Flow Solution

The boundary condition of flow tangency on the airfoil surface gives the integral equation:

$$\int_C K\gamma(s)ds + \gamma_L \left(\int_L Kds - \int_U Kds \right) + \vec{V}_\infty \cdot \vec{n} = V_N \qquad (3.8)$$

where the constant value of the strength of the lower free vorticity sheet is used and where the kernel function, K, is the normal velocity component (at the boundary point for which $\vec{V} \cdot \vec{n}$ is being enforced) due to a unit point vortex at the point associated with the element, δs, of the line of integration, and where the integraton paths, C, l and U, are the airfoil and the lower and upper free vortex sheet locations, respectively. The unknowns are the vorticity strengths on the curve, C, and on the free sheets represented by $\gamma(s)$ and γ_L, respectively. The former is a function of position on the airfoil, and the latter is a constant.

The right-hand side of Eqn. (3.8), V_N, is zero for the initial potential flow solution. Following a boundary layer analysis, however, the displacement effect is represented by a piecewise constant source distribution; V_N then becomes the integrated normal velocity induced by the boundary layer source distribution.

Numerical Solution

The airfoil contour is represented by an inscribed polygon, Figure 3. The individual panels representing the polygon each have a linear variation of vorticity across it. The free vortex sheets are represented by a number of panels of uniform vorticity. The value of the vorticity at the start of the ith panel is denoted by γ_i. Thus the function, $\gamma(s)$, in Eqn. (3.9) can be expressed in terms of the unknown sequence, $\{\gamma_i\}$, and the integral equations in the unknown function, $\gamma(s)$, become algebraic equations in the unknowns, $\{\gamma_i\}$. Initially there are $N+1$ unknown γ_i values (for N panels), but the auxiliary conditions remove two unknowns:

--at the upper surface separation point, $\gamma_{sep} = -\gamma_L$

  (γ_L being the value at the lower separation point),
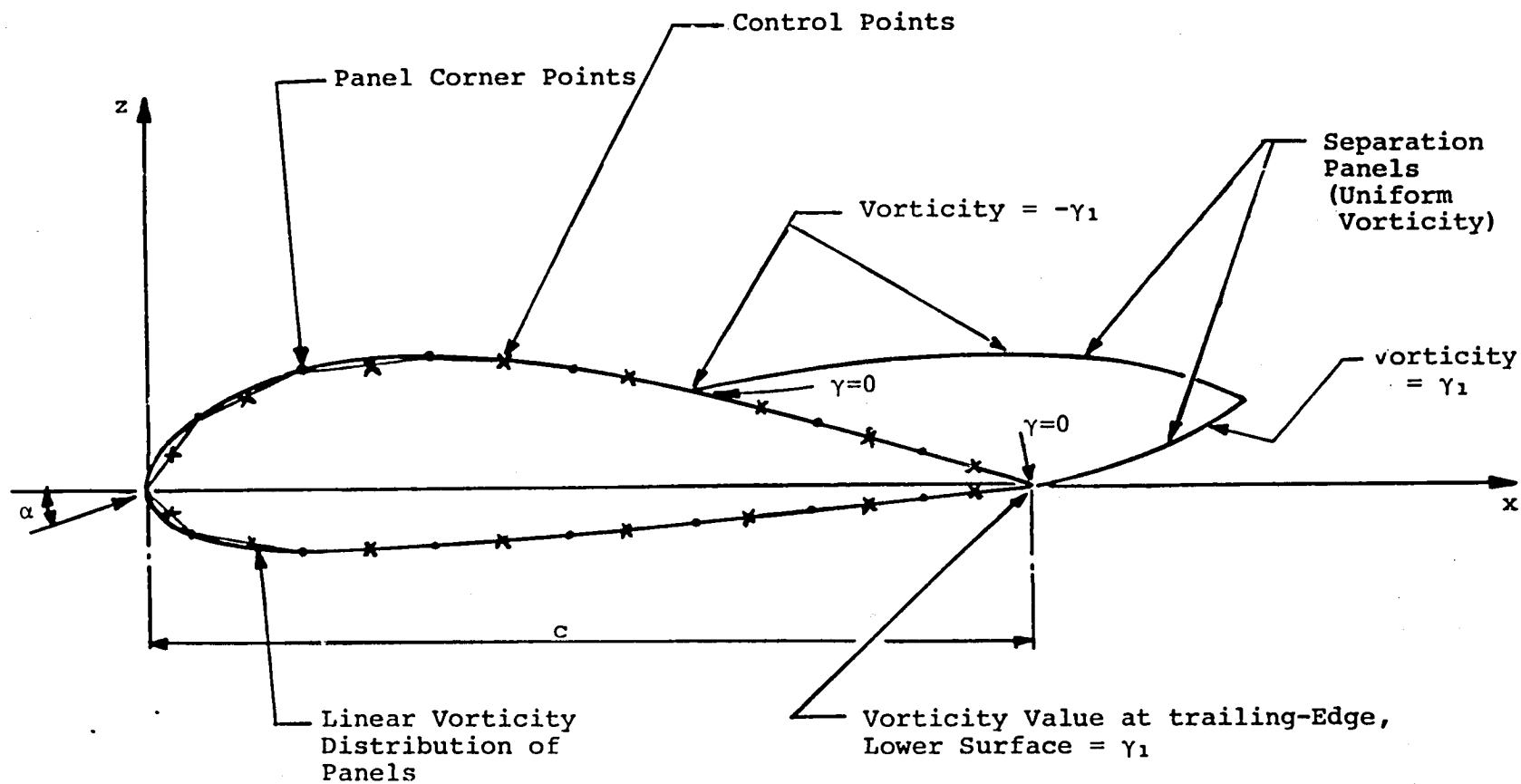
--and $\gamma_{N+1} = 0$.

14

FIGURE 3.   VORTICITY MODEL FOR THE POTENTIAL FLOW

Also, the γ value just downstream of the separation point on the upper surface is set to zero. Thus, there are N-1 unknown γ_i values. Enforcing the surface boundary condition (Eqn. (3.9)) at the panel midpoints (control points) gives N equations. A square set of algebraic equations is obtained by introducing one unknown source strength distributed uniformly around the airfoil surface. Being linear in the unknowns, the equations are amenable to solution.

Calculation of Pressures

Having found the vorticity, the velocity at any point in the flow field can be evaluated by adding to the free stream the velocities induced by the vorticity and source distributions. The pressures are calculated from the velocities according to the Bernoulli equation which is expressed non-dimensionally as

$$C_p = 1 - \left(\frac{V}{V_\infty} \right)^2 + \frac{\Delta H}{q_\infty} \tag{3.10}$$

where $C_p = \dfrac{p - p_\infty}{q_\infty}$, $q_\infty = \frac{1}{2}\rho V_\infty^2$, and ΔH = increase in total pressure over that at infinity. Note that $\Delta H = 0$ everywhere except in the wake region for which it was previously shown (Eqn. (3.8)) that $\Delta H = \rho \overline{V} \gamma_L$.

3.2.3 Structure of the Iterative Procedure

Figure 4 shows an outline of the method which has two iterative loops.

(1) Wake Shape Iteration

The iteration loop for wake shape is the inner loop and involves the potential flow analysis only. Although the vorticity is assumed to be a constant in the wake region, the free vortex sheets in the wake are divided into a number of panels to facilitate the computation of aerodynamic influence coefficients. The separation points within this iteration loop are fixed. The separation points may be located anywhere on a surface panel; they are not restricted to panel edge points.
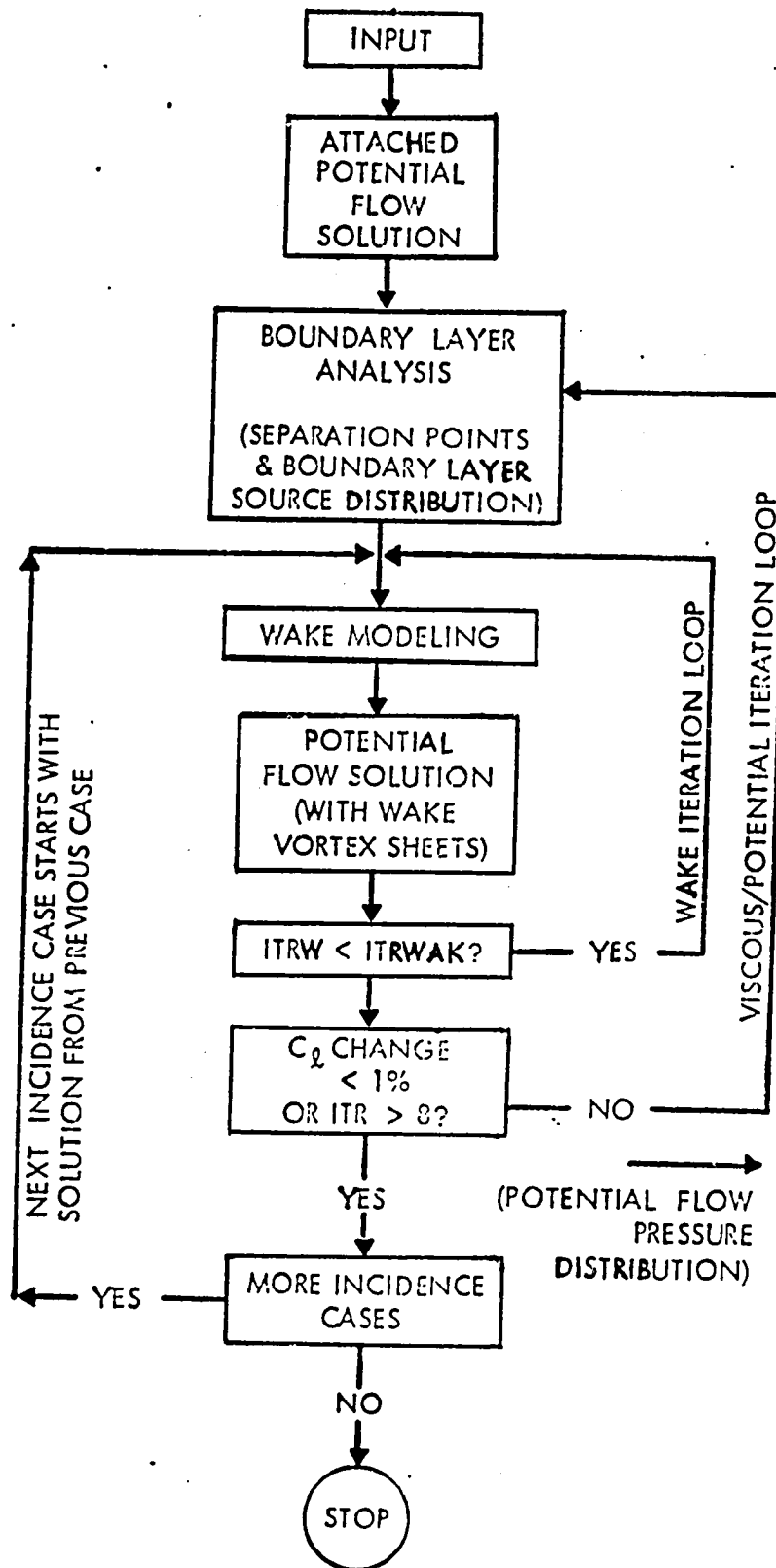
FIGURE 4.   PROGRAM OUTLINE

The wake shape is calculated as follows. Using the previous vorticity distribution, velocities are calculated at the panel midpoints on the free vortex sheets. The computed velocity distribution is then used to arrive at the new wake shape by re-orienting the wake panels in such a way they are tangential to the local flow directions, starting from the separation points.

The upper and lower sheet downstream end points, which were coincident in the initial wake, are allowed to move independently in subsequent iterations. At each iteration, the wake influence coefficients at the surface control points are recalculated, and a new potential flow solution is obtained.

(2) Viscous/Potential Flow Iteration

This outer iteration loop takes the potential flow pressure distribution over to the boundary layer analysis and returns with the separation points and with the boundary layer source distribution. The source distribution is determined directly from the boundary layer solution as

$$\sigma = \frac{d}{ds} (U_e \delta^*)$$

where U_e is the streamwise potential flow velocity at the edge of the boundary layer, and δ^* is the displacement thickness. The addition of this source distribution modifies the normal velocity, V_N (Eqn. (3.8)), at each panel control point. The sources are set to zero in the separated region.

The program generates a new wake shape using the new separation points together with information from the previous iterated wake. A new potential flow solution is then obtained, and so on. The outer iteration is terminated when the change in C_ℓ is below 1%. A limit of twelve iterations is currently imposed within the program.

4.0 MODIFICATION OF MCARF WITH SEPARATION FLOW MODEL (MCARFM)

The primary objective of the present work is to modify the MCARF program to accept the CLMAX free vortex sheet separation model. In this section, a description of this modification is presented.

For the present study, the program is capable of analyzing a multi-component configuration with separation only on one of the components, the trailing component. The major task of the present investigation involves the development of two iteration loops to incorporate the separation model in MCARF. The inner (wake) iteration loop for the potential flow relaxes the wake shape for a prescribed separation position, while the outer (viscous/potential flow) iteration loop predicts the separation point location and the displacement thickness distribution from the boundary layer analysis for each of the components. The concept of displacement thickness is used to represent the effect of the various viscous layers on the outer potential flow. In MCARF, the viscous effects of the boundary layer are simulated in the potential flow calculation by one of the following two options. In the first option (IPOT = 0), the displacement thickness is combined with the airfoil geometry to arrive at an equivalent airfoil geometry after each viscous/potential flow iteration. In the second option (IPOT = 1), instead of adding the displacement thickness to the airfoil geometry, a distribution of sources along the airfoil surface is utilized for the simulation of the viscous flow displacement effects. This is the so-called surface transpiration method which, within the framework of thin boundary layer theory, is completely equivalent to the method of adding geometrically the displacement thickness to the basic airfoil geometry. In the present investigation, the second option is used as it is convenient to adopt the separation flow model into MCARF.

4.1 Development of Separation Flow Model

The major code changes to model the separation flow model involve the modification of subroutine, POTVL, the potential flow solution routine in MCARF (Overlay 2). For the present investigation, the model is restricted to either a single component airfoil or to a multi-component airfoil with separation restricted to the trailing component only. The separation location over the upper surface (trailing component) is predicted from the boundary layer analysis, starting with the pressure distribution computed from the potential flow (attached or separated) solution in the previous iteration. It is assumed that the separation at the lower surface always occurs at the trailing-edge of the airfoil.

Initially, the streamlines are not known and so the shapes of the upper and lower surface free vortex sheets are represented by parabolic curves passing from the separation points to a common point downstream. The slope at the upstream end is the mean between the free stream direction and the local surface slope. The common point downstream is positioned on the mean wake line, distance WL downstream from the wake midpoint (Figure 2). The wake length is obtained by multiplying the height of the wake by the wake fineness ratio, WF, which is a function of airfoil section. For any given airfoil, a proper choice of WF can be input utilizing the experience gained while developing the AMI CLMAX program. (See Appendix)

4.2 Potential Flow Solution

For the airfoil with separation, the potential flow solution is obtained using the singularity distribution method of Oellers. The governing flow equation (3.2), and the details of the method were presented in Section 3.0. The airfoil surface is divided into N segments over each of which the vortex strength is assumed to be a constant. The free vortex sheets (separation region) are represented by a number of segments (NSEPWK) of uniform vorticity, the value of which at the upper surface separation point, $\gamma_{sep} = -\gamma_\ell$, with γ_ℓ as the value at the lower separation point. Sources are distributed along the airfoil surface to represent the displacement effect of the boundary layer. The stream function of the flow field includes the contribution of this source sheet.

In MCARF, the panel information, the coordinates of segment boundaries and midpoints, etc., are computed in routine AIRGM (Overlay 1). For a given airfoil the same panel information is used throughout the complete viscous/potential flow iterative scheme for an attached flow case. However, for a separated flow case, the separation point location where the upper surface vortex sheet leaves the airfoil surface is an arbitrary parameter which varies from one viscous/potential flow iteration to another iteration. In order to eliminate any flow distortions due to the presence of this upper separation point near the midpoint of any panel where the flow boundary conditions are satisfied, the region near the separation is repaneled in such a way that the upper surface separation point always coincides with a panel boundary. Also, the geometry of 3 panels on either side of the separation point is adjusted in such a way that they are uniformly spaced. This repaneling scheme is a temporary arrangement at each of the viscous/potential flow iterations, and the changed panel geometry is replaced with the original panel geometry before proceeding to the next iteration.

20

For the separation flow model, the modified Kutta condition (Eqn. (3.5)) of MCARF is replaced with the separation wake condition, $\gamma_{sep} = -\gamma_\ell$, and it is assumed that γ varies quadratically for the last four segment corners near the upper surface separation point and the lower surface trailing edge of the airfoil. Hence, the uniform vorticity (γ_{sep}) in the separation region is not an additional unknown in the system of equations consisting of N+1 unknown values of γ's (N) and ψ. Additionally, in the separation region, γ values just downstream of the separation point and at the upper surface trailing edge of the airfoil are assumed to be zero (see Figure 3).

In the present version of MCARF, the boundary conditions are satisfied by taking the difference between the stream function values at N-1 set of two adjacent segment midpoints, thereby eliminating the unknown value of stream function from the solution set. Hence for the attached flow case, the N-1 boundary conditions combined with the Kutta condition yield a consistent set of N equations with N unknown values of γ's on the N segments of the airfoil surface. For the separated flow case, a similar computational procedure is adopted with the following exceptions. The Kutta condition is satisfied for the separation wake region as discussed earlier in this section. The vorticity values on the downstream segment following the separation point and the trailing-edge segment on the upper surface are assumed to be zero. Hence two additional equations are eliminated from the original set of N equations to arrive at a consistent set of N-2 equations with N-2 unknown values of vorticity. As discussed earlier, γ_{sep} is not an additional unknown and is expressed as a function of the γ values at the four segments preceding the separation point. The pressure distribution in the separation region is computed using Eqn. (3.10).

4.3   Structure of the Iterative Scheme

The iterative scheme adopted in the present development is very similar to that of the CLMAX program (Figure 4), with a few exceptions. In the CLMAX program, it was assumed that a solution is converged at the iteration when C_ℓ changes less than 1% from the value at the previous iteration; however, the maximum number of iterations (ITRMAX) are limited to 8 due to the storage and data transfer limitations in the program. In the present program, ITRMAX can be input by the user, and it can be as high as any convergence criterion demands. In the original MCARF program, ITRMAX is assumed to be 10 with an additional restriction that the solution is assumed to be converged when C_ℓ is within 0.005 from the C_ℓ obtained in the previous iteration. Computations on several single and multi-element airfoil cases resulted in converged solutions after as few as 5 iterations.

21

4.3.1 Wake Shape (Inner) Iteration

The iterative loop for wake shape is the inner loop which involves the potential flow solution only. Within this loop, the upper surface separation point, which was computed from the boundary layer solution of the previous iteration, is fixed. Initially, the upper and lower vortex sheets are represented by parabolic curves and a potential flow solution is obtained as described earlier in this section. The upper and lower vortex sheets are divided into an equal number of panels (NSEPWK). NSEPWK is an input parameter and the suggested value for it is equal to or greater than the number of panels in the separation region over the upper surface of the airfoil. In the present program, NSEPWK is a single independent parameter; however, it can easily be modified into a variable parameter which is a function of the angle of attack.

A schematic of the wake iteration loop is presented in Figure 5. The wake shape is calculated as follows. Using the previous vorticity distribution, velocities are calculated at the panel midpoints on the free vortex sheets. The new wake shape is then determined by piecewise integration, starting at the separation points. The upper and lower sheet downstream end points, which were coincident in the initial wake, are allowed to move independently in subsequent iterations. At each iteration, the wake influence coefficients at the surface control points are recalculated, and a new potential flow solution is obtained.

The maximum number of iterations (ITRWMX) is an input parameter. Testing of several cases at different points of separation on a GA(W)-1 airfoil indicated that a maximum of three iterations is adequate to obtain a converged wake shape. Figure 6 presents iterated wake shapes on a GA(W)-1 airfoil at a fixed separation point (x/c = 0.5), and as can be seen, the wake shape is converged after only two iterations. In the present program, ITRWMX is fixed at 3; however, the user can change it if needed.

4.3.2 Viscous/Potential Flow (Outer) Iteration

The outer iteration loop takes the potential flow over to the boundary layer analysis and returns with the separation point over the upper surface of the last component and the boundary layer source distribution. Turbulent boundary layer analysis is performed using an incompressible integral method of Truckenbrodt (Ref. 10). In the present version of MCARF, the flow is assumed to separate at the location where the boundary layer shape factor (H) value exceeds HSEP. This is at best an engineering approximation. In a later version of MCARF a more reliable separation
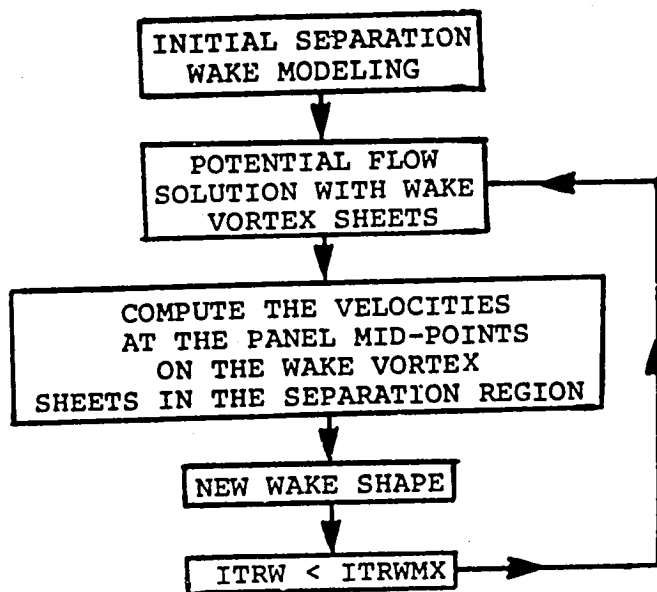
22

```
         ┌─────────────────────┐
         │ INITIAL SEPARATION  │
         │   WAKE MODELING     │
         └─────────────────────┘
                    │
                    ▼
         ┌─────────────────────┐◄──────────────┐
         │   POTENTIAL FLOW    │                │
         │ SOLUTION WITH WAKE  │                │
         │   VORTEX SHEETS     │                │
         └─────────────────────┘                │
                    │                           │
                    ▼                           │
      ┌───────────────────────────────┐         │
      │    COMPUTE THE VELOCITIES      │         │
      │   AT THE PANEL MID-POINTS      │         │
      │      ON THE WAKE VORTEX        │         │
      │ SHEETS IN THE SEPARATION REGION│         │
      └───────────────────────────────┘         │
                    │                           │
                    ▼                           │
           ┌─────────────────┐                  │
           │ NEW WAKE SHAPE  │                  │
           └─────────────────┘                  │
                    │                           │
                    ▼                           │
          ┌──────────────────┐                  │
          │ ITRW < ITRWMX    │──────────────────┘
          └──────────────────┘
```

FIGURE 5.   INNER(WAKE) ITERATION LOOP

23

Initial Wake

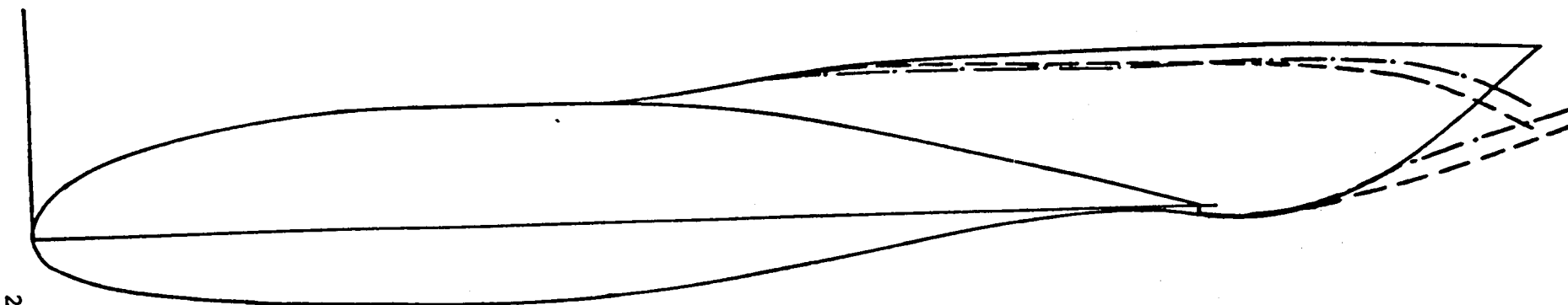—— — — First Iteration

—·—·— Second, Third, and Fourth Iterations

FIGURE 6.   SEPARATED WAKE ITERATIONS
GA(W)-1 AIRFOIL(XSEP/c = 0.5)

criterion of Nash and Hicks (Ref. 11) was incorporated in sub-routine TURB and it should be fairly simple to add this routine into the present MCARF program with the separation flow model. For the present investigation, the separation criterion of Truckenbrodt is used and an optimum value for HSEP is arrived at after an investigation of several test cases.

In the surface transpiration method adopted in the present investigation, a distribution of sources simulates the displacement effect of the viscous layers. The strength σ of this equivalent source is calculated from

$$\sigma = \frac{d}{ds} \left(\frac{\rho_e V_e \delta^*}{\rho_\infty V_\infty} \right) \tag{4.1}$$

where ρ is density, V is the velocity, s is the coordinate along the airfoil surface, δ^* is the displacement thickness, and e and ∞ refer to local and free-stream conditions, respectively. The local conditions are at the outer edge of the boundary layer. The addition of this source distribution modifies the normal velocity, V_N, at each control point. The sources are set to zero in the separation region.

The outer iteration scheme starts with the attached flow solution, the boundary layer analysis of which yields the upper surface separation point location and the boundary layer source distribution. Using this information, an initial wake shape is defined and the inner iteration procedure is followed to obtain the relaxed wake shape and the potential flow solution with separated wake. The boundary layer analysis for the separated flow yields a new set of the separation location and the boundary layer source distribution. This viscous/potential flow iterative process is repeated until a convergent solution is obtained. Figure 7 shows the history of the separation point and lift coefficient of a GA(W)-1 airfoil at an angle of attack of 19.06^0. This demonstrates a good convergence characteristics of the present model.

4.4 Discussion of Some Problems/Solutions

During the course of the present investigation, a major difficulty was encountered. While trying several viscous/potential flow iterations, it was discovered that the separation location over the upper surface continued to move towards the leading edge monotonically. A close look at the velocity distribution revealed that the velocity gradients and the shape factor, H, increased rather rapidly at the three panels forward of the separation region, which results in the prediction of the separation location always forward of the separation location from
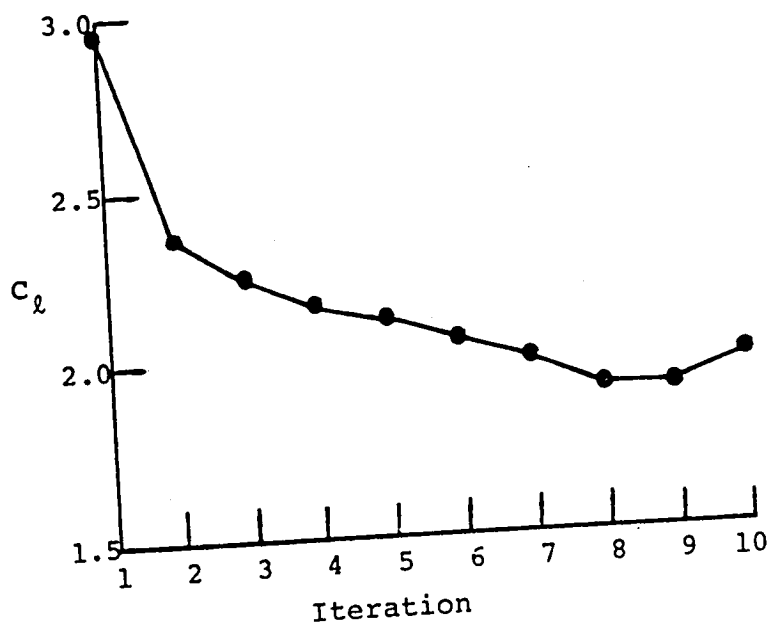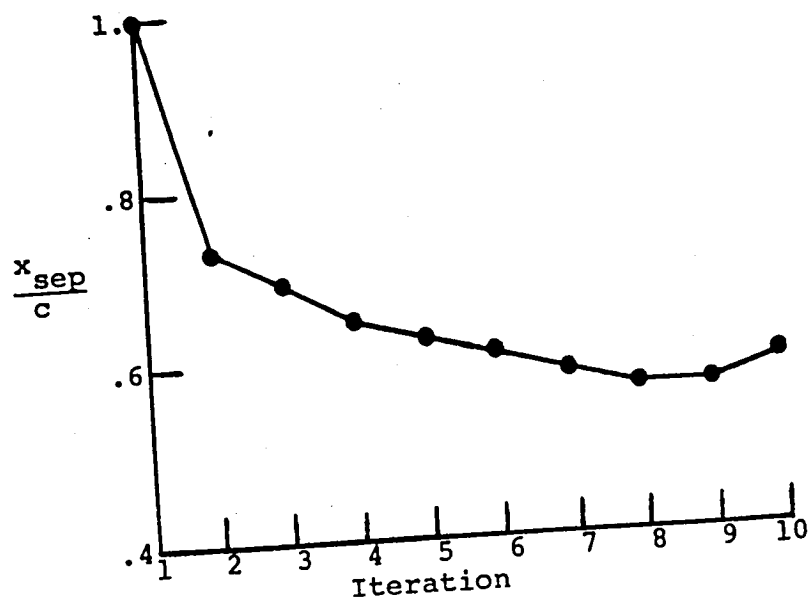
25

FIGURE 7. VISCOUS/POTENTIAL FLOW ITERATION CHARACTERISTICS
GA(W)-1 AIRFOIL($\alpha = 19.06^{\circ}$ and Re = 6.3 x 10^6)

the previous iteration, where the separated wake starts. It was first thought that this might be due to the present Kutta condition, which assumes that the vortex strengths vary quadratically for the last four segment corners near the upper surface location and the lower surface of the trailing edge and that the vortex strength in the separation wake, $\gamma_{sepu} = -\gamma_{sep\ell}$, the vortex strength at the lower surface trailing edge. Several other alternate Kutta conditions such as linear variation of vortex strength for the last two segment corners and constant vortex strength at the last segment near the upper surface separation location and the lower surface of the trailing edge were tried. These conditions alleviated the problem of steep rise in velocity gradients near the separation region somewhat, but did not eliminate it completely. Based on this investigation, it was concluded that this problem of rapid increase of velocity gradients may be due to the potential flow singularity model and the procedure adopted in the formulation of the aerodynamic matrix in MCARF. In MCARF, the tangential flow boundary conditions are satisfied by formulating a set of equations between pairs of two adjacent segment midpoints, thereby eliminating the unknown stream function value over the surface. While the model proved to be very effective for attached flows, it may require some modification for the proper handling of the separated flow and a more detailed and thorough investigation is needed to conclude whether it is indeed the problem.

In view of the time limitation in the present investigation, the problem of rapid increase of velocity gradients near the separation region and, hence, the continued shift of separation towards the leading edge of the airfoil, is solved by modifying the velocity distribution at the last two segments ahead of the separation region such that the gradients remain constant and are equal to the gradient at the third segment ahead of the separation region. This approach allowed the separation location to move forward as well as aft as the viscous/potential flow iterations progress in a physically consistent way. Admittedly, this modification is not justified on a purely scientific basis, but it is felt that it is a good engineering approximation, expecially supported by the experience gained while developing the AMI CLMAX program.

In the MCARF program, HSEP, the value of the boundary layer shape factor at which the flow separates, was assumed to be 1.8. In the present investigation, several separated flow cases (high angles of attack) were investigated varying the value of HSEP between 1.8 and 2.0 and it was concluded that the optimum value for HSEP = 1.85 based on the correlation between the computed and test results.

As discussed earlier in this section, the MCARF program has two options available for simulating the viscous effects. In the first option (IPOT = 0), the boundary layer displacement thickness is used to arrive at an equivalent airfoil geometry after each viscous/potential flow iteration. In the second option (IPOT = 1), the viscous effects are simulated by adding an appropriate source distribution along the airfoil surface. For the present separation flow modific tion, the second otpion is used. However, during the course of the present investigation, it was discovered that MCARF uses the first option only and the second option was not completely checked out. In fact, for a few cases investigated, it was found that the second option yielded substantially larger C_ℓ values for attached flows, while the results using the first option correlated well with the experiment. This discrepancy may be attributed to one or both of the following reasons: (i) the maximum allowable source strengths may be low; (ii) an inadequate representation of wake centerlines in the presence of the source distribution. This problem does not present any difficulty for separated flow, since the boundary layer calculation is terminated at the separation location and the source strengths are assumed to be zero in the separation region. Hence it is suggested to use option 1 for low angles of attack (with no separation), while it is required to use option 2 for separated flows. The appropriate changes are made in the present program (MCARFM) to incorporate this particular option.

5.0 DISCUSSION OF RESULTS

The method was applied to a single component GA(W)-1 and NACA 4412 airfoils. GA(W)-1 airfoil shape represents a difficult test case and pressure distributions are available from experiments at NASA-Langley for a range of angles of attack.

The first set of results, Figures 8-11, are for a GA(W)-1 airfoil at a Reynolds number of 6.3×10^6. Figure 8 shows a very good agreement between the calculated and experimental pressure distributions at $\alpha = 19.06°$ (which corresponds approximately to $C_{\ell_{max}}$). The calculation took ten viscous/potential flow iterations. The history of separation and lift coefficient for this case, which is shown in Figure 7, indicates a good convergence characteristic. Figure 9 compares the calculated and experimental pressure distributions at $\alpha = 20.05°$, which is just beyond the stall. Once again, there is good agreement. Figure 10 compares the calculated and experimental pressure distributions at $\alpha = 21.14°$. The comparison is not as good as the other cases because the predicted separation point has not reached the experimental value at about 0.1c. The rate of forward movement of the calculated separation point with 21.14° is slow. The sudden forward movement of the separation point in the experiment in just over a degree of change in angle of attack (compare Figures 9 and 10) is difficult to predict in this case.
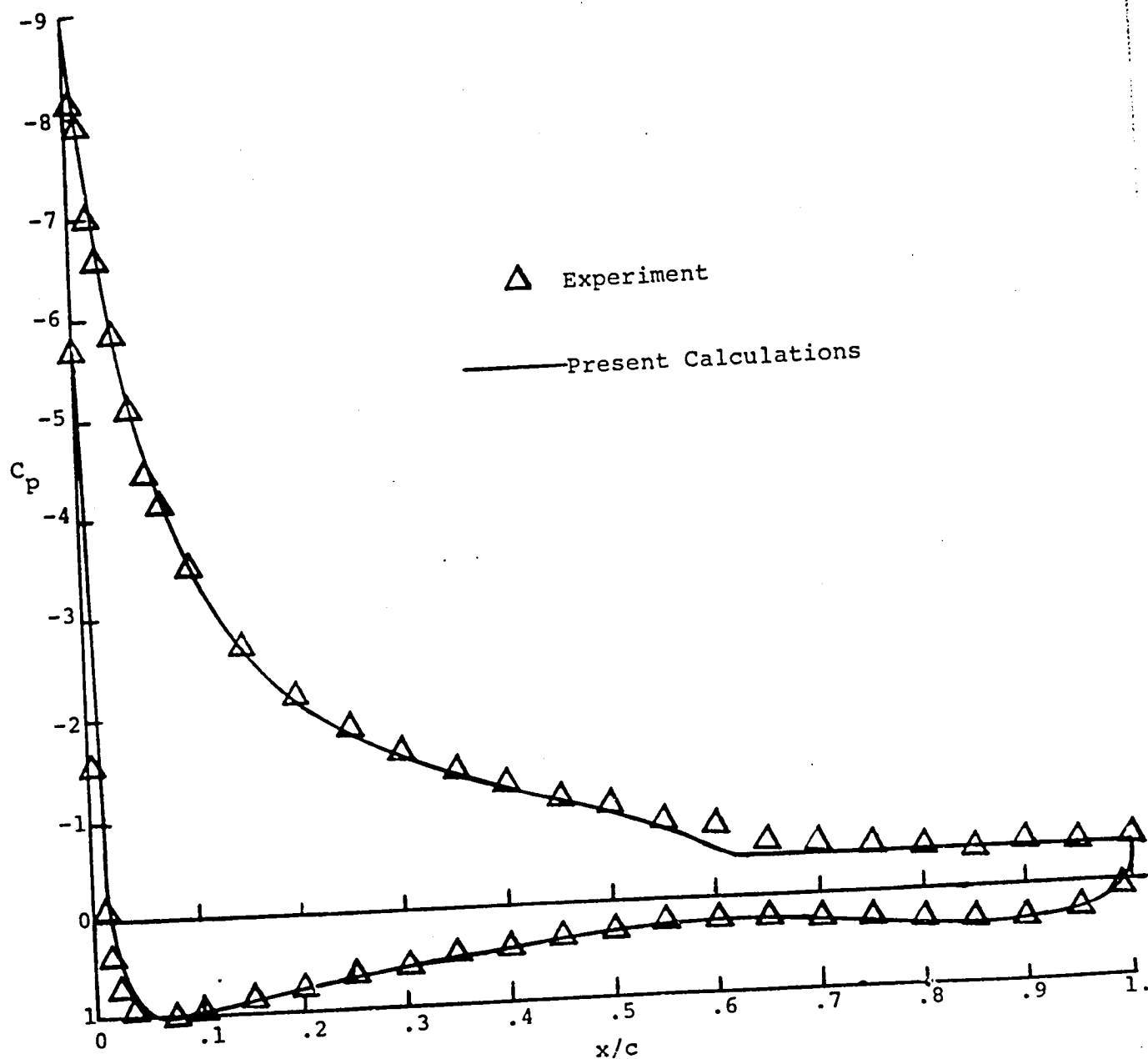
28

FIGURE 8. COMPARISON OF CALCULATED AND EXPERIMENTAL PRESSURE
DISTRIBUTION ON A GA(W)-1 AIRFOIL
(α = 19.06°, Re = 6.3 x 10^6, and M = 0.15)

29
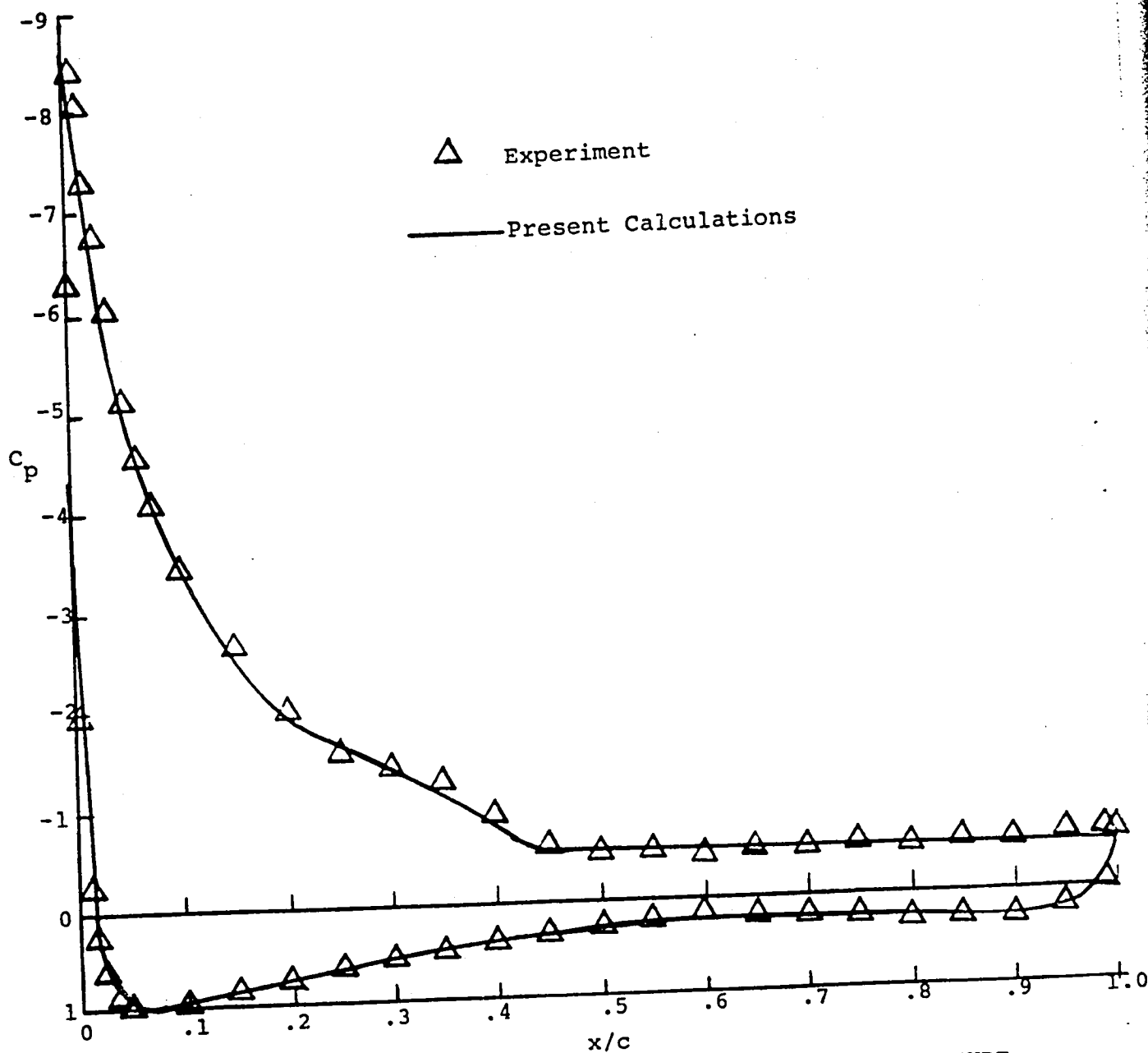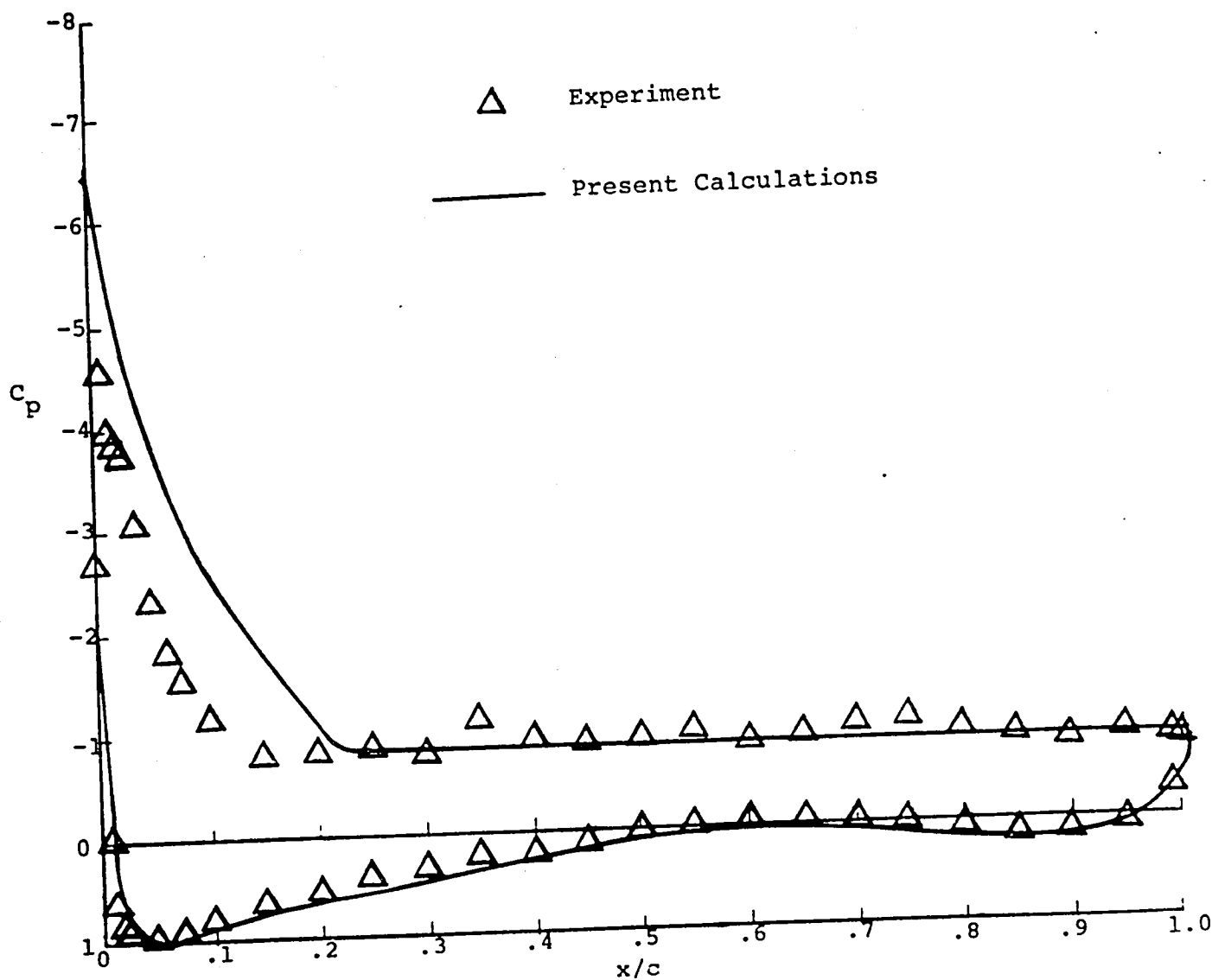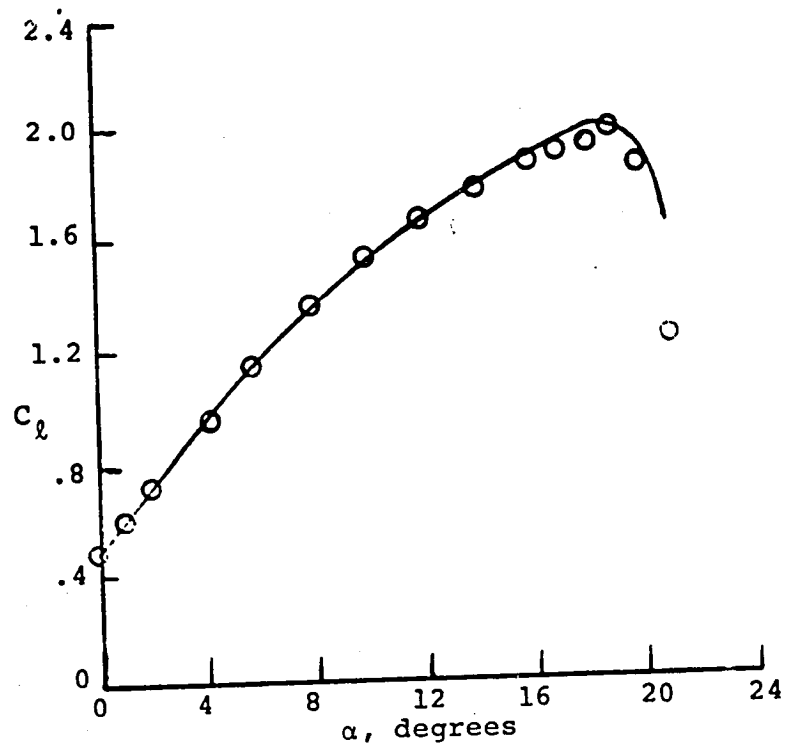
FIGURE 9. COMPARISON OF CALCULATED AND EXPERIMENTAL PRESSURE
DISTRIBUTION ON A GA(W)-1 AIRFOIL
($\alpha = 20.05°$, Re = 6.3×10^6, and M = 0.15)

30

FIGURE 10. COMPARISON OF CALCULATED AND EXPERIMENTAL PRESSURE DISTRIBUTION ON A GA(W)-1 AIRFOIL ($\alpha = 21.14°$, Re = 6.3 x 10^6, and M = 0.15)
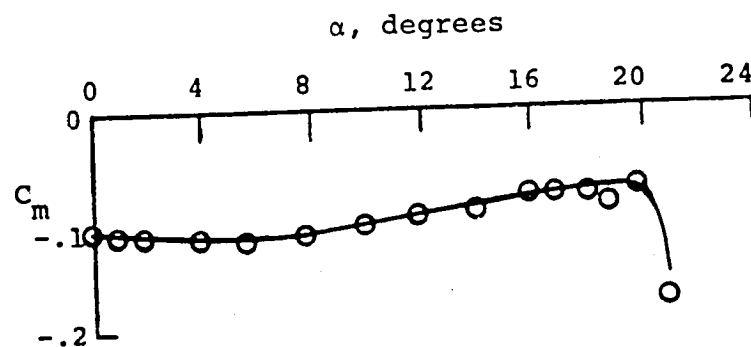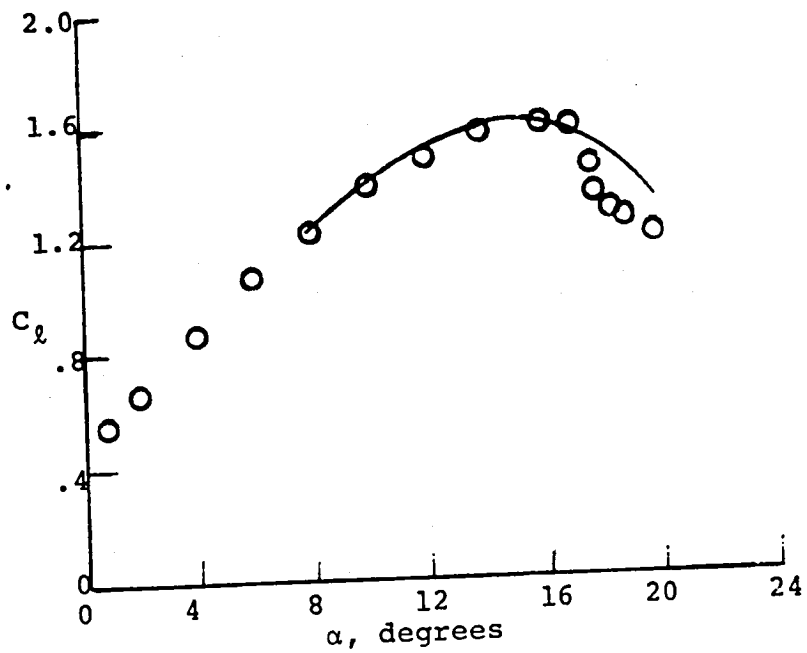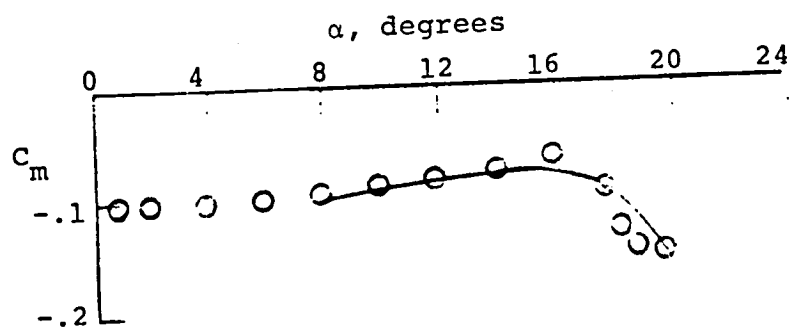
31

FIGURE 11. COMPARISONS OF CALCULATED AND EXPERIMENTAL LIFT AND PITCHING MOMENT CHARACTERISTICS FOR GA(W)-1 AIRFOIL (Re = 6.3×10^6 and M = 0.15)
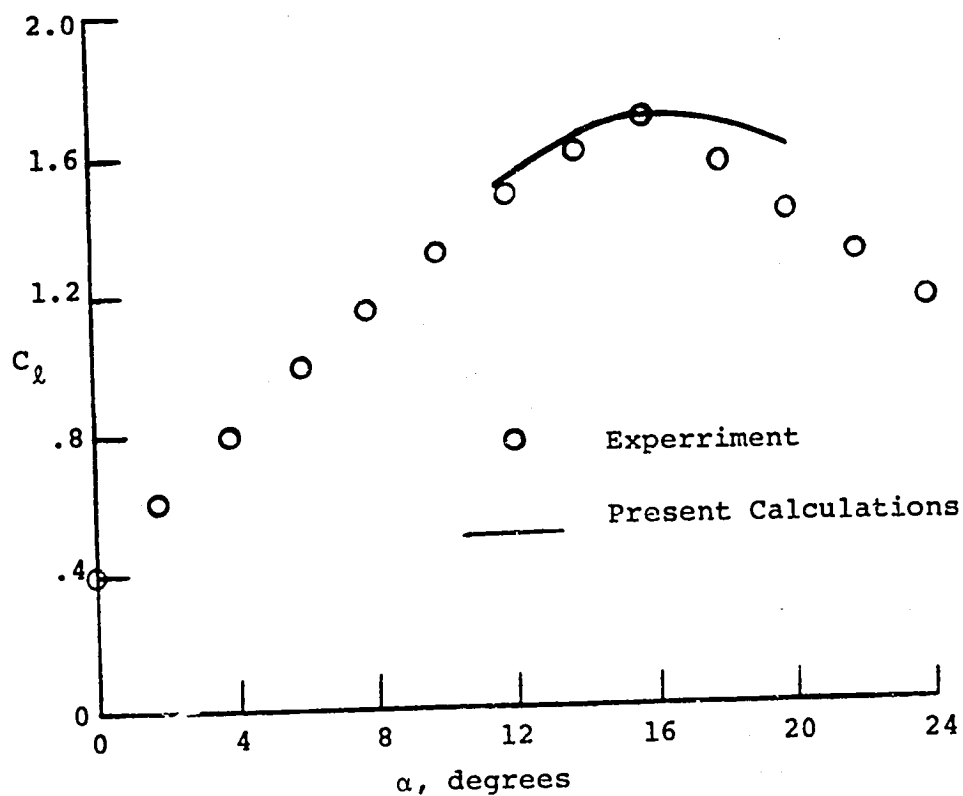
32

FIGURE 12. COMPARISONS OF CALCULATED AND EXPERIMENTAL
LIFT AND PITCHING MOMENT CHARACTERISTICS FOR
A GA(W)-1 AIRFOIL (Re = 2.1 x 10⁶ and M = o.15)

33

FIGURE 13.   COMPARISON OF CALCULATED AND EXPERIMENTAL
LIFT CHARACTERISTICS FOR A NACA 4412 AIRFOIL
(Re = 6.3 x 10^6)

34

Figures 11 and 12 show the lift and moment characteristics of the GA(W)-1 airfoil at Reynolds numbers 6.3×10^6 and 2.1×10^6, respectively. As can be seen from these figures, they show good agreement with experiment. Figure 13 shows the lift coefficient comparison with experiment (reference 12), for a NACA 4412 airfoil at Re = 6.3×10^6. The calculated values agree very closely with the experimental values up to $C_{\ell_{max}}$.

In all of the cases studied under the present investigation, the calculated values compare well with the results of the AMI CLMAX program.

6.0 CONCLUSIONS

The separation flow model incorporated into MCARF has been applied to single component airfoils. Calculated pressure distributions for angles of attack up to the stall are in close agreement with experimental measurements. Even at higher angles of attack beyond the stall, correct trends of separation, decrease in lift coefficients, and increase in pitching moment coefficients are predicted.

Although the program is designed to handle multi-component airfoils with separation at the trailing component only, multi-component airfoils have not been checked out. It is suggested a better separation criterion such as the method of Nash and Hicks be incorporated into the model as opposed to the present method of Truckenbrodt.

7.0 REFERENCES

1. Morgan, Harry L., Jr., "A Computer Program for the Analysis of Multi-Element Airfoils in Two-Dimensional Subsonic, Viscous Flow", NASA SP-347, Part II, pp. 713-454, 1975.

2. Jacob, K., "Computation of Separated Incompressible Flow Around Airfoils and Determination of Maximum Lift", AVA Report 67A,62, 1967.

3. Barnwell, R.W., "Two Inviscid Computation Simulations of Separated Flow about Airfoils", AIAA Paper No. 76-379; July 1976.

4. Carlson, L.A., "Inverse Transonic Airfoil Design Methods Including Boundary Layer and Viscous Interactions Effects", TAMRF Report No. 3224-77-02, May 1977.

5. Maskew, B. and Dvork, F.A., "The Prediction of $C\ell_{max}$ Using a Separated Flow Model", AHS Journal, April 1978.

6. Oellers, H.J., "Incompressible Potential Flow in a Plane Cascade Stage", NASA TT F-13, 982, 1971.

7. Goradia, S. H., "Confluent Boundary Layer Flow Development with Arbitrary Pressure Distribution", Ph.D. Thesis, Georgia Institute of Technology, 1971.

8. Cohen, C.B. and Reshotko, E., "The Compressible Laminar Boundary Layer with Heat Transfer and Arbitrary Pressure Gradient', NACA Report 1294, 1956.

9. Schlichting, H., Boundary Layer Theory, McGraw-Hill Book Co., Inc., 1968.

10. Truckenbrodt, E., "A Method of Quadrature for Calculation of the Laminar and Turbulent Boundary Layer in Case of Plane and Rotationally Symmetrical Flow", NACA TM 1379, 1955.

11. Nash, J.F. and Hicks, J.G., "An Integral Method Including the Effect of Upstream History on the Turbulent Shear Stress," Proceedings Computation of Turbulent Boundary Layers -- 1968 AFOSR-IFP Stanford Conference, Vol. 1, Stanford University Dept. of Mech. Eng., Stanford, Calif.

12. Pinkerton, R.N., "The Variation with Reynolds Number of Pressure Distribution over an Airfoil Section", NACA Report No. 613, July 1937.

APPENDIX: PROGRAM PARAMETERS

In the present separation flow model, one of the important parameters is the wake fineness ratio (WF--see the discussion in Section 3.2.1). While developing the AMI CLMAX program, a range of airfoil sections and thickness ratios were tested. The dependence of WF on airfoil thickness/chord ratio is presented in Figure 14. This data is used as a reference guide for the present investigation.

The input parameters and the format for the present program (MCARFM) is identical with the input of MCARF with the exception of the first card (CARD A), which is read from the MAIN program (Overlay 0). The input variables and the format specification on CARD A are presented below.

CARD A: Separation Flow Variables

Column	Variable	Description	Format
1-5	NSEPWK	Number of panels in the separation region	I5
6-10	ITRWMX	Maximum number of wake shape iterations	I5
11-20	WF	Wake fineness ratio	F10.0
21-30	HSEP	The value of boundary layer shape factor at which the flow is assumed to separate	F10.0

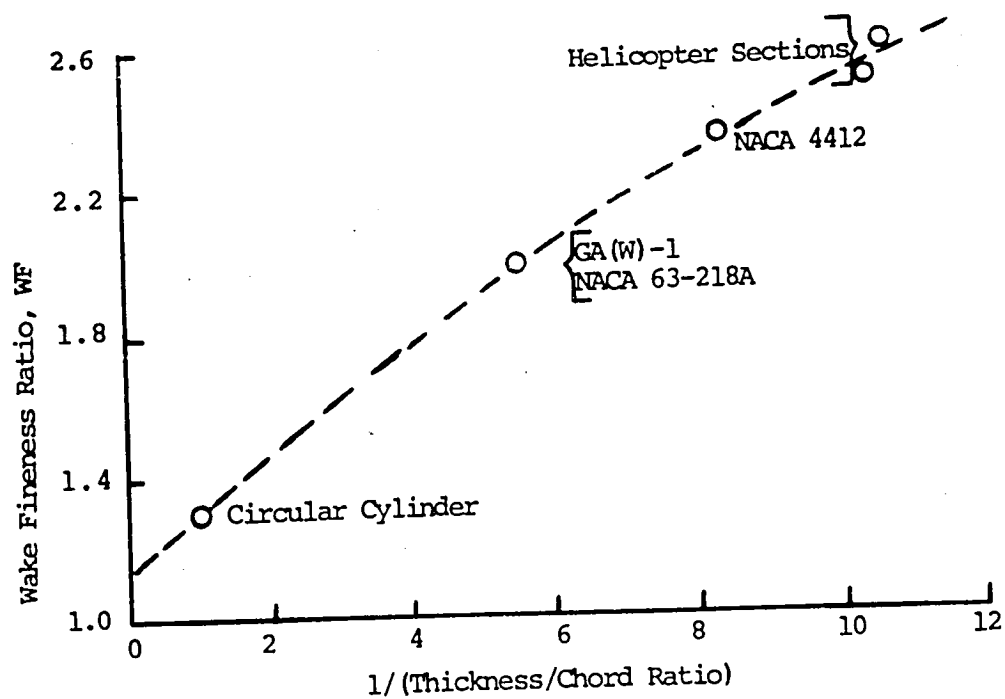Wake Length = WF x Wake Height (see Figure 2)

FIGURE 14. DEPENDENCE OF WAKE FINENESS RATIO, WF, ON AIRFOIL THICKNESS/CHORD RATIO.

38

End of Document